ELSEVIER

Journal of Electron Spectroscopy and Related Phenomena 126 (2002) 133–144

JOURNAL OF ELECTRON SPECTROSCOPY and Related Phenomena

www.elsevier.com/locate/elspec

Photemission and the influence of collective excitations

Peter D. Johnson

Physics Department, Brookhaven National Laboratory, Upton, NY, USA

Abstract

The development of new capabilities in high resolution photoemission is allowing detailed studies of the role of collective many-body excitations in the decay of a photohole. This in turn provides new insights into the physics of condensed matter systems, in particular the strongly-correlated systems, which exhibit a rich variety of exotic phenomena including high Tc superconductivity.

Keywords: Photoemission; Collective excitations; Superconductivity; Self Energy

1. Introduction

The past three decades have seen the widespread use of photoemission as a probe of the electronic structure of a variety of materials [1]. Neville Smith and coworkers have played an integral role in the development of the technique. One important contribution was the demonstration that by measuring the photoemission spectrum as a function of angle, the technique could be used to map out the bulk electronic band structure [2]. Because of the relatively short mean free path of the photoelectrons, the technique has also been used extensively to study the properties of surfaces and thin films. In the former, the emphasis has been on studies of the unique electronic structure associated with the solid–vacuum interface [3]; in the latter, studies have followed the evolution of the electronic structure from monolayer thin films through to thicknesses resembling the bulk [4]. With the addition of spin detection, photoemission has been applied to the study of the spin dependent electronic states in magnetic surfaces and thin films [5]. Further, as discussed elsewhere in this volume [6], by measuring the intensities of the photoemitted electrons as a function of angle and kinetic energy, the techniques, photoelectron diffraction and holography, have been developed as a probe of atomic structure. Both Neville [7] and Chuck Fadley [8] played a role in the latter developments.

In photoelectron spectroscopy, a photon of known energy, ω, is absorbed and the outgoing electron's energy $(\omega - \varepsilon_k)$ and momentum are measured. These properties determine the energy ε_k and momentum $\underline{k}$ of the hole state left in the occupied valence bands [1]. Interaction effects, including for instance Coulomb and electron–phonon, cause the sharp line spectrum Im $1/(\omega - \varepsilon_k - i\eta)$ of independent electron theory to evolve into Im $1/(\omega - \varepsilon_k - \Sigma(\underline{k},\omega))$ where the complex self-energy $\Sigma(\underline{k},\omega)$ contains the effects of the many body interactions. The real part $\Sigma_1(\underline{k},\omega) \sim -\omega\lambda_k$ gives a shift in energy and associated mass enhancement, while the imaginary part

E-mail address: pdj@bnl.gov (P.D. Johnson).

0368-2048/02/$ – see front matter
PII: S0368-2048(02)00148-2

$\Sigma_2(\underline{k},\omega) = \Gamma_k(\omega,T)$ gives the lifetime broadening $\hbar/2\tau_k$. τ_k is the typical time before the hole state $\underline{k}$ scatters into other states $\underline{k}'$. The single-particle spectral function of the hole-state, $A(\underline{k},\omega) = (-1/\pi)G(\underline{k},\omega)$ takes the form

$$A(\underline{k},\omega) = \frac{\sum_2(\underline{k},\omega)}{[\omega - \varepsilon_k - \sum_1(\underline{k},\omega)]^2 + [\sum_2(\underline{k},\omega)]^2} \qquad (1)$$

New developments in instrumentation have recently allowed photoemission measurements to be performed with very high energy and momentum resolution [9]. This in turn has allowed detailed studies of the self-energy corrections to the lifetime and mass of excitations in the vicinity of the Fermi level. These developments come at an opportune time. Indeed the recent discovery of high temperature superconductivity in strongly correlated electron systems is presenting a range of challenges for condensed matter physics [10]. Does the mechanism of high Tc superconductivity represent new physics? Do we need to go beyond Landau's concept of the Fermi liquid [11]? Is there any evidence for the presence of quasiparticles in the excitation spectra of these complex oxides?

In this paper we review some of the developments with a particular reference to recent studies of the cuprates. In order to gain insight into the observations from such materials it is often useful to draw comparisons with other less complex systems. As such we also discuss photoemission studies of many body interactions in metallic systems.

2. Many body interactions in metallic systems

Photoemission represents a direct transition between an initial and final state. The transition results in a peak broadened to a width reflecting contributions from both the finite lifetime of the photohole and the momentum broadening of the photoelectron. The width Γ is given by [12]

$$\Gamma\left(\Gamma_h + \frac{\nu_h}{\nu_e}\Gamma_e\right)\left(\left|1 - \frac{\nu_h}{\nu_e}\right|\right)^{-1} \qquad (2)$$

where Γ_h is the width of the hole state, Γ_e is the width of the electron state and ν_h and ν_e are the respective perpendicular velocities. In a two dimensional system with $v_h = 0$, the width of the photoemission peak is therefore determined entirely by the width of the photohole, Γ_h. The observation that the width of the photoemission peak is determined solely by the lifetime of the photohole offers the possibility that the technique may be used as a probe of the scattering mechanisms contributing to the electrical transport in different materials. Unlike other probes of these transport properties, photoemission has the advantage that it is momentum resolving. However in drawing conclusions from such studies, it is important to remember that the single particle scattering rate measured in photoemission is not identical to the scattering rate measured in transport studies. The two are approximately related however and with certain assumptions, the transport scattering rate can be written $\hbar/\tau_{tr} = \hbar/\tau(1 - \cos\vartheta)$ where $\hbar/\tau$ represents the single particle scattering rate [13].

The intensity $I(\underline{k},\omega)$ measured as a result of the photoemission process is given by

$$I(\underline{k},\omega) = |M|^2 A(\underline{k},\omega) f(\omega) \qquad (3)$$

where M represents the matrix element linking the initial and final states and $f(\omega)$ is the Fermi function which enters because the photoemission process is restricted to excitation from occupied states below the Fermi level. Fig. 1 shows an image of the spectral intensity excited from a two-dimensional surface resonance in the $\bar{\Gamma} - \bar{N}$ azimuth of a Mo(110) crystal [14]. In the vicinity of the Fermi level, we note a change in the rate of dispersion, or mass enhancement, and a rapid change in the width of the band. The latter broadening reflects three principal contributions, electron–electron scattering, electron–phonon scattering and electron–impurity scattering. These different contributions all add linearly to give the total scattering rate Γ such that

$$\Gamma = \Gamma_{e-e} + \Gamma_{e-ph} + \Gamma_{imp} \qquad (4)$$

In a Fermi liquid the electron–electron scattering term is given by $\Gamma_{e-e}(\omega,T) = 2\beta[(\pi k_B T)^2 + \omega^2]$ where, within the Born approximation, $2\beta = (\pi U^2)/(2W^3)$. U represents the on-site Coulomb repulsion and W the bandwidth of the state. The electron–phonon contribution may be calculated via the Eliashberg equation such that [15]

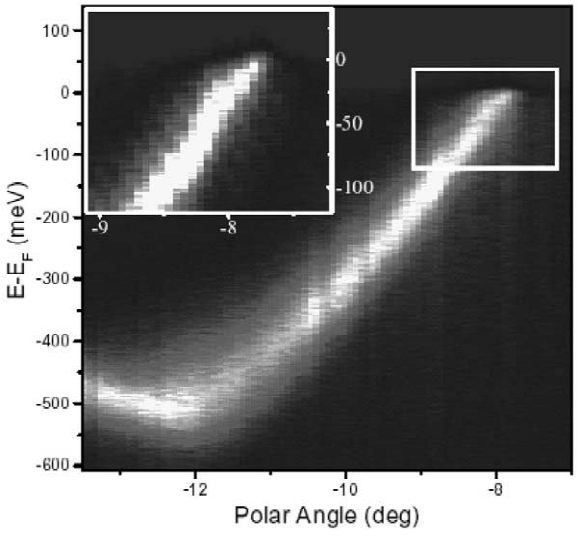

Fig. 1. ARPES intensity plot of the Mo(110) surface recorded along the $\bar{\Gamma}-\bar{N}$ line of the surface Brillouin zone at 70 K. Shown in the inset is the spectrum of the region around k_F recorded with particular attention paid to the surface cleanliness.

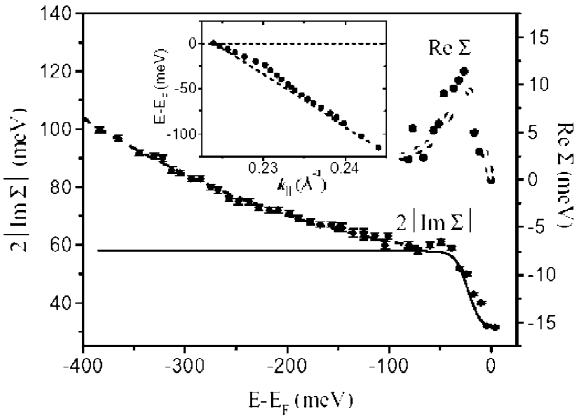

Fig. 2. The photohole self-energy for Mo as a function of binding energy at 70 K. The real part is obtained from the dispersion shown in the inset. The imaginary part is obtained from the width of the quasiparticle peak. The dashed line is a quadratic fit to the high-binding energy data ($\omega<-80$ meV). The dark (gray) solid line shows the calculated electron–phonon contribution to the imaginary (real) part of the self-energy. The calculated imaginary component is shifted up by 26 meV.

$$\Gamma_{\mathrm{e-ph}}(\omega,T)=2\pi\hbar\int_0^{\omega_0}\mathrm{d}\omega'\alpha^2F(\omega')[2n(\omega')+f(\omega'+\omega)+f(\omega'-\omega)]. \quad (5)$$

Here α^2F is the Eliashberg coupling constant and $f(\omega)$ and $n(\omega)$ are the Fermi and Bose–Einstein functions, respectively. $\Gamma_{\mathrm{e-ph}}$ increases monotonically with energy up to some cut-off defined by the Debye energy. At $T=0$ K the electron–phonon coupling constant is given by [16]

$$\lambda=2\int_0^{\omega_0}\frac{\alpha^2F(\omega')}{\omega'}\mathrm{d}\omega' \quad (6)$$

Above approximately one-third the Debye energy, $\Gamma_{\mathrm{e-ph}}(\omega,T)$ shows a linear temperature dependence with a slope given by $2\pi\lambda k_{\mathrm{B}}$. This latter observation has been the basis of several experimental determinations of λ [17]. The final contribution in Eq. (4), impurity scattering, is elastic in that the impurity atoms are considered to have no internal excitations. Thus the scattering-rate, Γ_{imp}, is proportional to the impurity concentration, but independent of energy and temperature. At sufficiently low temperature, impurity scattering represents the dominant decay mechanism for a hole close to E_F in any real system.

Fig. 2 shows the measured Im Σ or Σ_2 of the Mo surface state as a function of binding energy. The data points are extracted from the image of Fig. 1 in two ways, either from energy distribution curves (EDCs) or from momentum distribution curves (MDCs) [18]. In the former, EDCs, the photoemitted intensity is measured as a function of binding energy at constant angle or momentum. The width of a peak, ΔE, is related to the self-energy by

$$\Delta E\approx\frac{2|\sum_2(\omega)|}{1-\partial\sum_1(\omega)/\partial\omega}. \quad (7)$$

In MDCs the photoemitted intensity is measured as a function of momentum at constant binding energy. The width of the peak is then given by $\Delta k=2|\Sigma_2(\omega)|/\nu_F^0$ where ν_F^0 represents the bare or non-interacting velocity. In the vicinity of the Fermi level, coupling to low energy excitations can complicate the extraction of self energies from EDCs via Eq. (7) because of the strong energy dependence of Σ_1. The rapidly changing background reflecting the Fermi cut-off can add further complications. The

MDC approach is thus the preferred method of analysis for dispersing states close to E_F.

The calculated electron–phonon contribution to the self-energy is shown in Fig. 2. In the vicinity of the Fermi level, the agreement between the calculation using the theoretical α^2F of bulk molybdenum [19] and the experimentally measured widths is excellent. At binding energies greater than the Debye energy the electron–phonon contribution saturates. However, also shown in the figure is a quadratic fit to the measured widths at the higher binding energies. The quadratic dependence is an indication that electron–electron scattering, as in a Fermi liquid, plays an important role. The fit is consistent with the prefactor in the expression for Γ_{e-e} having $U \approx 0.6$ eV, as predicted for molybdenum [20], and $W \approx 1.3$ eV, the approximate bandwidth of the surface state. The measured widths also have an energy-independent contribution due to scattering from hydrogen impurity centers [14].

In magnetic systems the possibility also exists for scattering from magnetic excitations. This possibility has been examined in studies of ferromagnetic gadolinium. The results of this study are illustrated in Fig. 3 which shows the spin-polarized photoemission spectra recorded from a surface state on the Gd(0001) surface held at $T = 20$ K. Earlier experiments [21,22] and calculations [23] indicate that the surface state should be 100% majority spin, due to parallel alignment of the surface and bulk moments. The coexistence of both spin components at the same energy is therefore thought to be an intrinsic property of the surface state arising from a combination of spin–orbit and spin exchange processes as discussed by Nolting and coworkers [24].

Fitting the spectra in Fig. 3 with lorentzian line shapes shows that the minority spin peak has a larger width than its majority spin counterpart, 116 meV as opposed to 86 meV. Removing the contribution from the experimental resolution, these widths become approximately 105 meV in the minority spin channel and 70 meV in the majority channel. All scattering mechanisms give distinct spin dependent contributions to the total scattering rate. Electron–electron scattering by exchange processes favors the two holes in the final state being of opposite spin [25]. From consideration of the spin-dependent densities

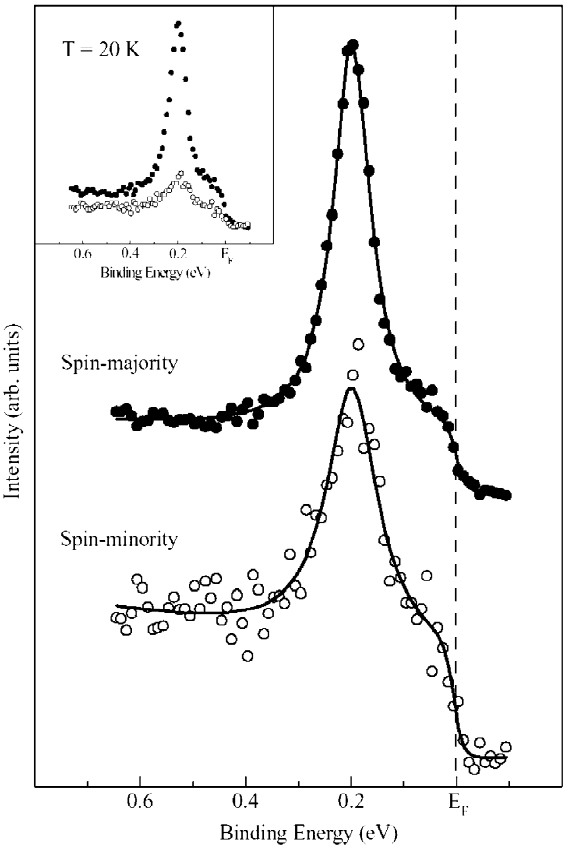

Fig. 3. Spin-resolved photoemission spectra recorded from the Gd(0001) surface at 20 K. The upper and lower spectra represent the emission in the majority and minority spin channels, respectively. The lines indicate Lorentzian fits to the spectra superimposed on appropriate backgrounds. The inset shows the relative intensities in the two spin channels.

of states, the scattering rate for this process is therefore estimated to be equal for majority and minority spin holes. The electron–phonon and impurity scattering rate are proportional to the density of states at the hole binding energy for the same spin while the electron–magnon or spin–flip scattering rate is proportional to the density of states for the opposite spin. As the majority-spin density of states is large and the minority-spin component small, impurity and electron–phonon scattering should be most important in the majority spin channel and less important in the minority spin channel. The fact that

the minority spin channel in Fig. 3 is broader indicates a mechanism involving the opposite spin such as electron–magnon scattering. Thus at $T=0$ K, the minority-spin component of the photohole can scatter to the majority-spin component elsewhere in the surface band by emitting a spin wave. The corresponding spin–flip process is not available to the majority-spin component of the photohole at $T=0$ because the localized f-spins have a saturated magnetization. At higher temperatures, inelastic scattering can occur back and forth between the two spin channels mediated by the emission or absorption of magnons.

In an approximate treatment [26] using the 's–f' Hamiltonian [27] Allen found the result

$$\hbar/\tau(\downarrow) = \frac{\sqrt{3}}{4}\frac{P'(\uparrow)m^*}{S}\left(\frac{2JSa}{\hbar}\right)^2 \quad (8)$$

for the decay of the minority ($\downarrow$) spin component due to spin flip scattering with magnon emission. Here J is the s–f exchange parameter giving the exchange splitting $2JS = 0.65$ measured for the surface state [28], $m^* = 1.21$ is the effective mass measured for the surface band, and $P'(\uparrow) = 0.87$ is the experimentally measured majority component of the band. With $S = 7/2$ and $a = 3.6$ Å, $\hbar/\tau(\downarrow) \approx 0.095$ eV. Conversely, replacement of $P'(\uparrow)$ by $P'(\downarrow) = 1 - P'(\uparrow)$ gave $\hbar/\tau(\downarrow) = 0.014$ eV for the majority spin component. Thus at low T, the majority spin channel is dominated by electron–phonon scattering whereas the minority spin channel is dominated by electron–magnon scattering. Based on the relative spin-dependent densities of states we can provide estimates of the contribution of phonon scattering in the two spin channels. These would be 46 meV in the majority spin channel and 10 meV in the minority spin channel. We are then left with approximately 10 meV in each channel due to impurity scattering, probably from hydrogen as in the case of molybdenum discussed previously.

It is interesting to note that when looking at unoccupied states the converse should be true. Thus at low temperatures, an electron added to an unoccupied minority spin band should decay preferentially via phonon scattering and an additional excited electron in a majority spin band should decay preferentially via magnon scattering.

3. Many body effects in high Tc superconductors

3.1. The normal state

It is well established that conventional superconductivity reflects the formation of bosons or Cooper pairs through the exchange of phonons between quasiparticles [29]. It is less clear that such a mechanism can be responsible for the high transition temperatures observed in high Tc superconductors. Indeed it has generally been assumed that the electron–phonon mechanism cannot support transition temperatures above approximately 30 K [10]. This view has been called into question in studies of superconductivity in field doped lattice expanded C_{60} films where transition temperatures as high as 117 K have been observed [30]. Further, it has recently been demonstrated that anisotropic phonon coupling can account for the relatively high Tc of 39 K observed in the new superconductor MgB_2 [31].

The situation is complicated in the field of high Tc superconductivity where, as demonstrated in early studies of the temperature dependence of the resistivity, the cuprates do not show the usual characteristics of a Fermi liquid. In a two-dimensional system, the resistivity $\rho \propto (k_F l)^{-1}$ with k_F is the Fermi wavevector and l is the mean free path between scattering events. In early studies of the cuprates, the resistivity was found to increase linearly through the Ioffe–Regel limit, the limit at which the mean free path is equal to the interatomic distance, and to continue increasing linearly to very high temperatures [32]. The latter observation can be taken as evidence for the lack of well-defined quasiparticles in a Fermi liquid as we have been discussing in the case of metallic systems. Indeed metals show a tendency for the resistivity to saturate at higher temperatures in the vicinity of the Ioffe–Regel limit.

Studies of the binding energy and temperature dependence of the photoemission linewidths clearly indicate non-Fermi liquid behavior in the normal state of the cuprates [30]. Fig. 4 shows measurements of the imaginary component of the self-energy for different temperatures in a study of optimally doped $Bi_2Sr_2CaCu_2O_{8+\delta}$ (Tc = 91 K) [18]. 'Optimal doping' is reference to the fact that the material is

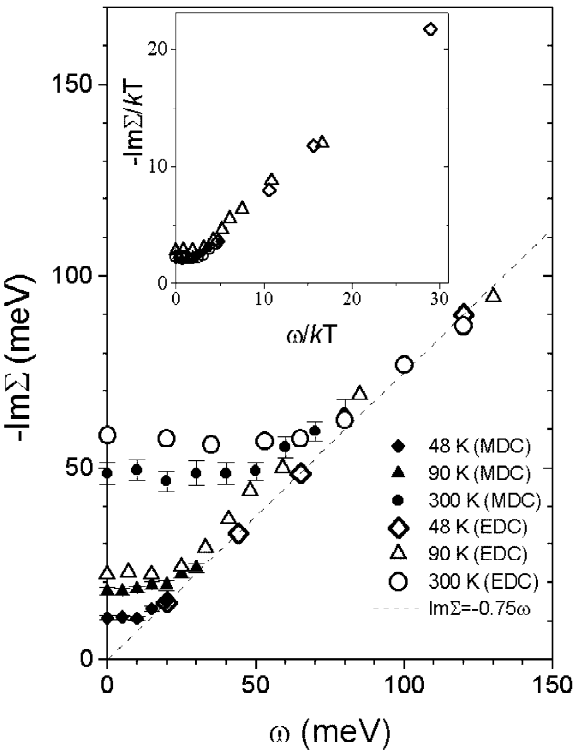

Fig. 4. A compilation of Im Σ for optimally doped $Bi_2Sr_2CaCu_2O_{8+\delta}$ obtained via Δk cuts or MDCs and from peak widths in EDCs as a function of binding energy for three different temperatures. The different temperatures are respectively; 48 K (diamonds), 90 K (triangles) and 300 K (circles). The different metods of analysis are in all cases indicated by filled symbols for MDCs and open symbols for EDCs. The inset shows the same data plotted in dimensionless units confirming the scaling behavior.

doped with carriers to a concentration giving the maximum superconducting transition temperature, T_c. The measurements, which were made along the 'nodal' direction, the direction where there is no observable gap in the superconducting state, show an interesting property. The imaginary component of the self-energy, Σ_2, is linear in binding energy when the binding energy is greater than the temperature and linear in temperature when the temperature is greater than the binding energy. This behavior, predicted in early non-Fermi liquid models of the high Tc superconductors [33,34], differs markedly from that of a Fermi liquid, which, as discussed earlier, is quadratic in both temperature and binding energy.

The linear frequency dependence of Σ_2 which results in Σ_1 taking the form $\omega \ln \omega_c/\omega$ with ω_c some cutoff frequency [34] implies an absence of quasiparticles in that the coherence factor of the latter is given by $Z = (1 - \partial\Sigma_1/\partial\omega)^{-1}$. The absence of coherent excitations is highlighted if we compare directly the measurements from the cuprate with those from molybdenum. Indeed in a Fermi liquid the inverse lifetime of a well-defined quasiparticle should be less than it's binding energy or $\hbar/\tau < \omega$. In Fig. 5, a comparison of Σ_2 obtained from the measured linewidths shows that the Mo displays characteristic Fermi liquid behavior but the cuprate does not. Thus if we have no coherent excitations in the normal state of the cuprates, what do we have? Several theories propose a mechanism whereby an excitation in the system breaks down into collective excitations, one chargeless excitation carrying away the spin, a spinon, and one spinless excitation carrying away the charge, a holon [35]. Such a decay mode is known to exist in one-dimensional systems [36]. However whether or not it exists in two-dimensional systems is still an open question. Shown in Fig. 6, the spinon excitation in a one-dimensional half-filled anti-ferromagnetic chain may be thought of as a local domain wall. Shown in the same figure, the spin flip excitation reflecting the absorption or

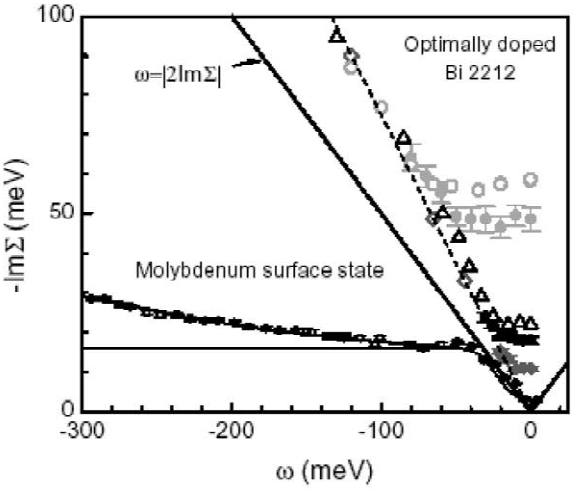

Fig. 5. A comparison of the measured imaginary component of the self energy, Σ'', for molybdenum and the optimally doped cuprate. The diagonal defines the condition by which $2\Sigma'' = E_b$ where E_b represents the binding energy of the excitation.

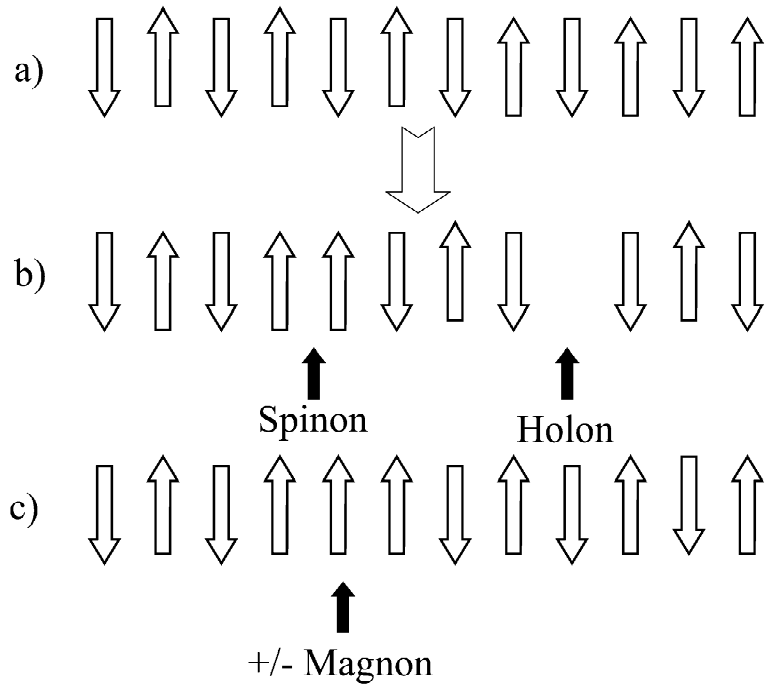

Fig. 6. (a) One-dimensional antiferromagnetic spin chain in ground state. (b) Photohole decays into chargeless excitation, the spinon, and a spinless excitation carrying charge, the holon. (c) Spin–flip excitation corresponding to the emission or adsorption of a magnon.

emission of a magnon corresponds to two spinon excitations.

In the study of Valla et al. [18] it was noted that in the nodal direction there existed a 'kink' in the band dispersion or mass enhancement in the vicinity of the Fermi level. The origin of this kink which exists over much of the Fermi surface [37] has recently become the subject of considerable interest. Indeed Lanzara et al. [38] have speculated that the mass enhancement reflects the coupling of quasiparticles to phonons as observed in the study of molybdenum discussed earlier and in related studies of beryllium [39]. The authors arrived at this conclusion based on the observation that the kink is observed at a similar binding energy in all of the cuprates and at a similar energy to that observed for the longitudinal optical phonons in inelastic neutron scattering studies [40].

The suggestion that excitations or quasiparticles in the vicinty of the Fermi level are renormalized through interaction with phonons is incompatible with the observation that the materials are non-Fermi liquids and hence characterized by a lack of quasiparticles. However it is of interest to explore the suggestion further. Let us consider coupling to an Einstein mode of energy 70 meV corresponding to the kink energy. Replacing α^2F in Eq. (5), the Eliashberg equation, with a δ-function representing the Einstein mode, we calculate the scattering rate as a function of binding energy. As shown in Fig. 7, at low temperatures the scattering rate shows a step function at the mode energy that broadens as the temperature is raised. The step function in Σ_2, which is to be expected in that at 0 K, Eq. (1) reduces to $\Sigma_2 = \pi\hbar \int_0^{|\omega|} d\omega' \alpha^2 F(\omega')$, will result, via the Kramers–Kronig transform, in a cusp in Σ_1 or a 'kink' in the dispersion at a similar binding energy. The presence of thermally excited phonons of energy 70 meV, which corresponds to a temperature of 840 K, does not start to become obvious until temperatures of the order of room temperature or above are reached.

In contrast to these calculated scattering rates, both photoemission studies [18,37] and IR studies [41] indicate that the scattering rate is entirely linear

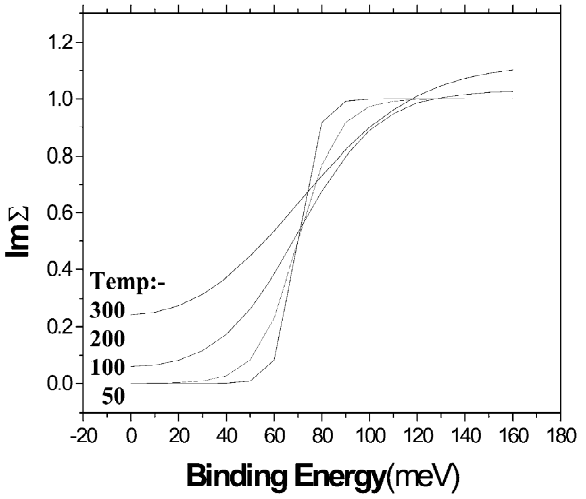

Fig. 7. Calculated scattering rates (Im Σ) as a function of binding energy for different temperatures as indicated. The calculations reflect coupling to a discrete Einstein mode of energy 70 meV.

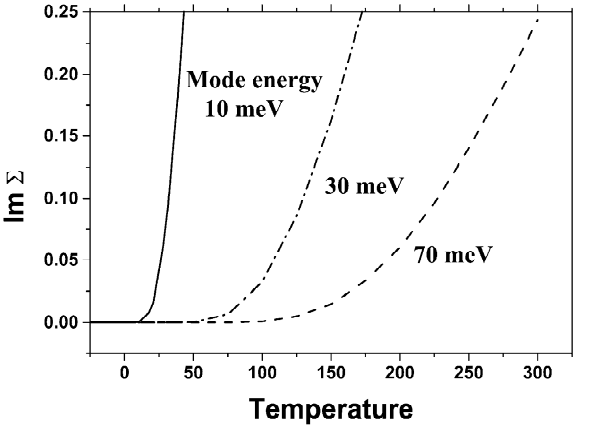

Fig. 8. Calculated temperature dependence of Im Σ at E_F reflecting coupling to Einstein modes of different energies as indicated.

in frequency for temperatures in the range 150 K and above. The observation of a linear scattering rate at temperatures as low as 150 K is a strong indication that that there is no structure in α^2F, i.e. that there is no experimental evidence of coupling to an Einstein mode in the vicinity of 70 meV. As the temperature is lowered, the IR studies indicate that the scattering rate deviates from the linear behavior. However any deviation at the lower temperatures can be associated with the onset of the superconducting state.

It is also of interest to examine the temperature dependence of the scattering rates at the Fermi level. At low temperatures a photohole created at the Fermi level can only decay through an electron at higher binding energy absorbing a phonon. It cannot decay through the emission of a phonon. This is illustrated in Fig. 8 where we show calculated scattering rates for a hole at E_F interacting with Einstein modes of different energies. As we discussed earlier, above a temperature of approximately one-third the mode energy the scattering rates become linear in temperature. However it is also important to note that as the energy of the mode increases, its effect on the scattering rate does not become apparent until higher and higher temperatures. Put simply, at low temperatures there is not enough thermal energy to excite the mode. Fig. 9 shows a compilation of temperature dependent momentum widths (inverse mean free paths) measured along the nodal direction in a number of different experiments. All clearly show a marked temperature dependence even at low temperatures. This is an indication that if the temperature dependence is a reflection of quasiparticles coupling to phonons, the Debye enrergy is of the order of 25 meV or less, i.e. too low produce a kink in the dispersion in the range 50–80 meV. Rather it suggests that the temperature dependence is dominated by some other form of scattering, possibly electron–electron.

It is important to note that the above description in terms of the Eliashberg equation requires the presence of quasiparticles in the normal state. Our analysis has shown that the experimental observations are inconsistent with such a model. In an alternative analysis, consistent with the absence of quasiparticles, one simply recognises, as noted earlier, that the Kramers–Kronig transform of a scattering rate linear in frequency results in the real part of the self-energy taking the form $\Sigma_1 = \omega \ln \omega_c/\omega$ [34]. It is unclear as to what value should be assigned to ω_c. However it is clear that, without ever invoking the need for coupling to some form of collective mode, the logarithmic correction implies a deviation from linear dispersion in the vicinity of E_F. It is also true however that in these strongly correlated sys-

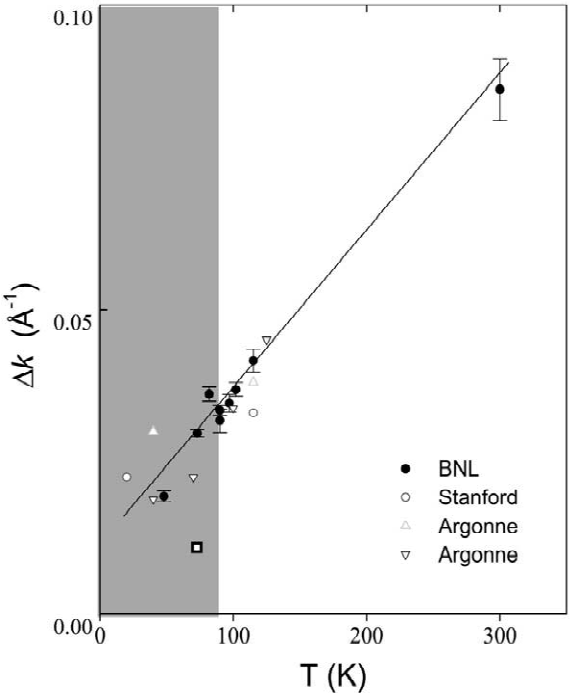

Fig. 9. The measured temperature dependent momentum widths or inverse mean free paths in the nodal direction of the high Tc superconductor, $Bi_2Sr_2CaCu_2O_{8+\delta}$. Also shown is the measured momentum width of the molybdenum surface state discussed in Ref. [14]. The latter presumably provides an indication of the current experimental resolution limitation in these studies. The high Tc data are taken from from different experiments as indicated. The BNL data is taken from Ref. [18], the Stanford data from Ref. [37] (a), Argonne[1] from Ref. [37] (b) and Argonne[2] from Ref. [47]. In the latter case Δk is determined from the measured FWHM of the EDCs and ν_F.

tems, the excitations, whatever they may be, probably have some vibrational component in them.

3.2. The superconducting state

Photoemission studies of the cuprate $Bi_2Sr_2CaCu_2O_{8+\delta}$ show that the dispersion in the nodal direction in the vicinity of the Fermi level is modified again as the system enters the superconducting state [42]. This effect is more pronounced in the underdoped region as indicated in Fig. 10. Indeed in the overdoped regime there is no measurable change between the normal and superconducting states.

Fig. 11 shows the temperature dependence of the difference or change in dispersion as a function of temperature for a sample with transition temperature 70 K. The difference is measured at a binding energy at which the maximum difference is measured at low temperatures. Also shown in the figure is the temperature dependence observed for a magnetic mode observed in $Yba_2Cu_3O_{6+x}$, a related cuprate with identical Tc, by inelastic neutron scattering [43]. The mode is associated with a singlet to triplet excitation in the spin excitation spectrum. Both phenomena in Fig. 11 clearly show an identical temperature dependence that can be associated with the onset of superconductivity. It has recently been suggested [44] that the mode cannot be responsible for the dispersion anomalies observed in photoemission [42,45] or in infra-red spectroscopy [41]. This is because the mode is known to represent only a small component of the total spectral intensity $2g^2\mu_B^2S(S+1)$. Further the coupling is calculated to be small. However it should be noted that both of these latter assertions are still the subject of ongoing debate [46].

The mode reflecting the underlying long range antiferromagnetic order has a wavevector $Q(\pi,\pi)$. Examination of Fig. 12 shows that coupling to such a mode will be strongest in the vicinity of 'hot' spots in the anti-nodal region. Several groups have noted that in the superconducting state the measured Fermi velocity, ν_F, shows a continuous reduction on moving from the nodal region around the Fermi surface to the anti-nodal region [38,47,48]. The measured velocity is related to the bare velocity, ν_0, such that $\nu_F = \nu_0(1+\lambda)^{-1}$. Thus the observation of a reduced velocity is consistent with the possibility of increased coupling. It is also clear on the basis of Fig. 12, that any coupling in the nodal direction will become stronger as the doping is reduced and the Fermi surface approaches that characteristic of the half-filled antiferromagnetic insulator. Such an increase has indeed been reported in several studies [38,42]. It seems reasonable therefore to associate the behavior observed in the photoemission with the spin degrees of freedom. However even though there appears evidence invoking the mode as the source of any dispersion anomalies it is important to note that the superconductivity does not reflect some BCS like

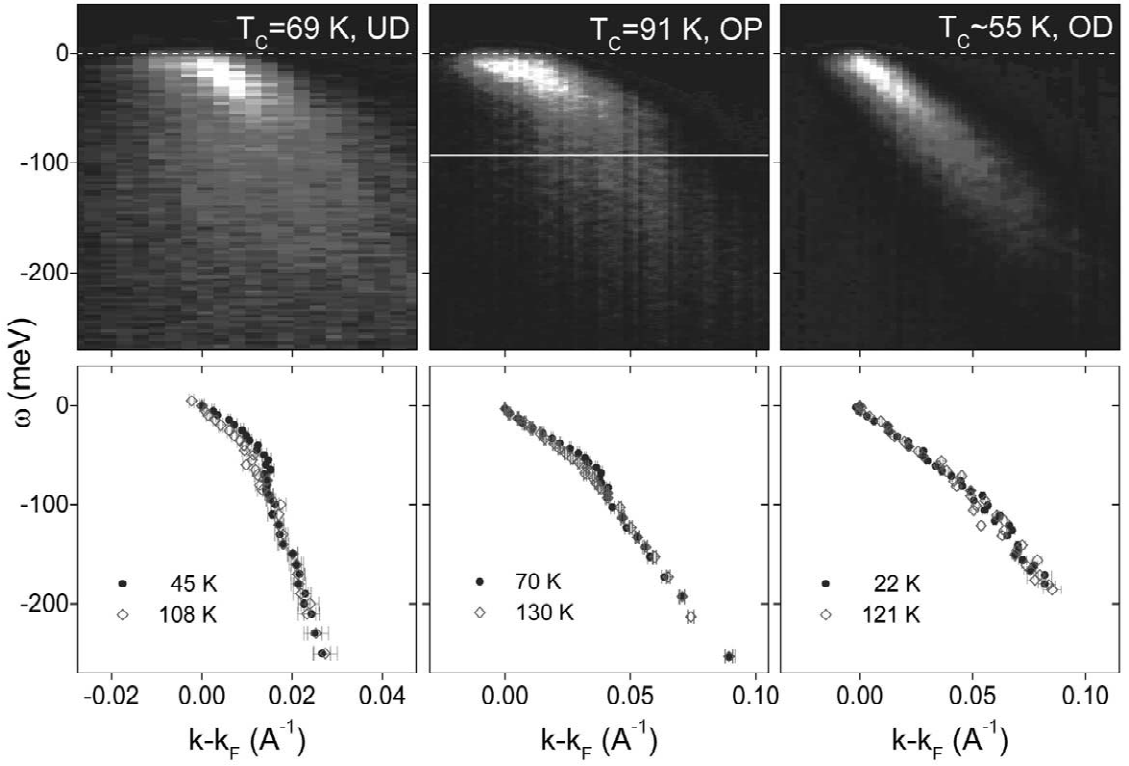

Fig. 10. Upper panels: Two dimensional photoemission intensities observed from (a) underdoped (UD), (b) optimally doped (OP) and (c) overdoped (OD) $Bi_2Sr_2CaCu_2O_{8+\delta}$ samples. The superconducting transition temperatures are indicated. Lower panels: The dotted lines indicate the MDC deduced dispersions for both the superconducting (blue dots) and normal states (open red diamonds) corresponding to the different samples in the panels above.

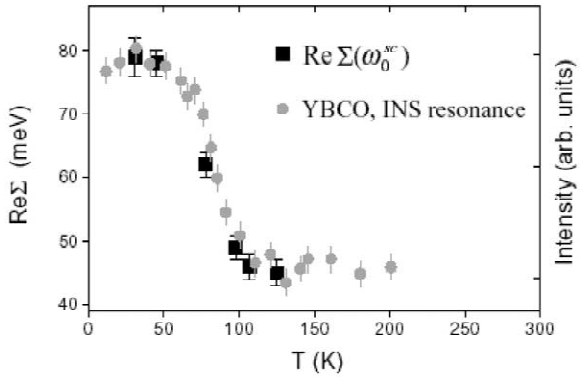

Fig. 11. Temperature dependence of Re $\Sigma(\omega_0^{sc})$ from the nodal line for the UD69 K sample (open squares) compared with the temperature dependence of the intensity of the commensurate resonance mode observed in neutron scattering studies of underdoped $YBa_2Cu_3O_{6+x}$ ($T_{c=74\ K}$).

mechanism with the mode serving as the boson. Rather it is generally concluded that the presence of the mode reflects the formation of the superconducting state rather than the cause of the superconducting state.

Acknowledgements

Much of the work discussed in this article reflects discussion and collaboration with T. Valla, A. Fedorov, B.O. Wells, Z. Yusof, S. L. Hulbert, G. Gu, N. Koshizuka, P.B. Allen, Q. Li, A. Moodenbaugh and many others. However it is also a pleasure to acknowledge the many years of collaboration with Neville Smith who has proved an invaluable source of information on the many intricacies of electronic structure and photoemission. Work at Brookhaven

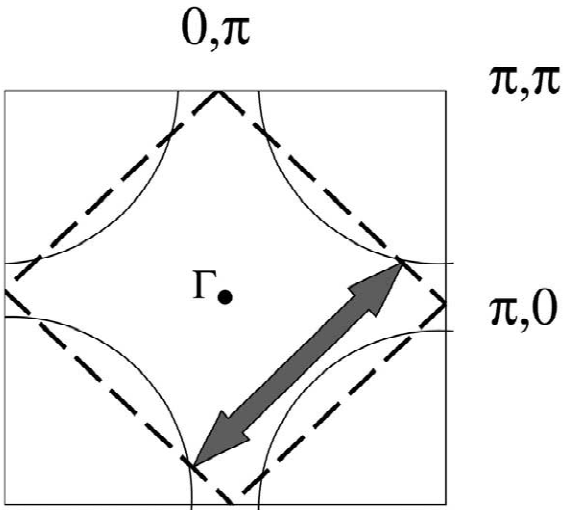

Fig. 12. Fermi surface of a half-filled antiferromagnetic insulator (dashed line) compared with Fermi surface of the doped system (solid arcs). Hot spots are joined by the double ended arrow representing the magnetic mode with wave-vector (π,π).

National Laboratory is supported by the Department of Energy under contract number DE-AC02-98CH10886

References

[1] S.D. Kevan (Ed.), Angle-Resolved Photoemission, Elsevier, Amsterdam, 1992.
[2] N.V. Smith, M.M. Traum, F.J. Disalvo, Solid State Commun. 15 (1974) 211.
[3] S.D. Kevan, W.E. Eberhardt, in: S.D. Kevan ((Ed.), Angle-Resolved Photoemission, Elsevier, Amsterdam, 1992.
[4] T. Miller, T.-C. Chiang, J. Elect. Spectros. Relat. Phenom. 117–118 (2001) 413.
[5] P.D. Johnson, Rep. Prog. Phys. 60 (1997) 1217.
[6] D.P. Woodruff, (2002) Vol. 126/1–3. X-ref.: PII: S0368-2048(02)00205-0.
[7] D.P. Woodruff, D. Norman, B.W. Holland, N.V. Smith, H.H. Farrell, M.M. Traum, Phys. Rev. Lett. 41 (1978) 1565.
[8] C.S. Fadley, M.A. Van Hove, A. Kaduwela, S. Omori, L. Zhao, S. Marchesini, J. Phys.: Cond. Matt. 13 (2001) 10517.
[9] G. Beamson, D. Briggs, S.F. Davis, I.W. Fleicher, D.T. Clark, J. Howard, U. Gelius, B. Wannberg, P. Baltzer, Surf. Interf. Anal. 15 (1990) 541.
[10] P.W. Anderson, The Theory of Superconductivity in the High-Tc Cuprates, Princeton University Press, Prineton, NJ, 1997.
[11] L.D. Landau, J. Exp. Theoret. Phys. (USSR) 30 (1956) 1058.
[12] N.V. Smith, P. Thiry, Y. Petroff, Phys. Rev. B 47 (1993) 15476.
[13] N.V. Smith, Phys. Rev. B 64 (2001) 155106.
[14] T. Valla, A.V. Fedorov, P.D. Johnson, S.L. Hulbert, Phys. Rev. Lett. 83 (1999) 2085.
[15] G.D. Mahan, Many Particle Physics, Plenum Press, New York, 1990.
[16] G. Grimvall, The Electron–Phonon Interaction in Metals, North-Holland, New York, 1981.
[17] B.A. Mcdougall, T. Balasubramanian, E. Jensen, Phys. Rev. B 51 (1995) 13891.
[18] T. Valla, A.V. Fedorov, P.D. Johnson, B.O. Wells, S.L. Hulbert, Q. Li, G.D. Gu, N. Koshizuka, Science 285 (1999) 2110.
[19] S.Y. Savrason, D.Y. Savrason, Phys. Rev. B 55 (1997) 10895.
[20] W.A. Harrison, Electronic Structure and the Properties of Solids, W.H. Freeman and Co, San Francisco, CA, 1980.
[21] G.A. Mulhollan, K. Garrison, J.L. Erskine, Phys. Rev. Lett. 69 (1992) 3240.
[22] D. Li, J. Zhang, P.A. Dowben, K. Garrison, P.D. Johnson, H. Tang, T.G. Walker, H. Hopster, J.C. Scott, D. Weller, D.P. Pappas, Mat. Res. Socs Proc. 313 (1993) 451.
[23] D.M. Bylander, L. Kleinman, Phys. Rev. B 50 (1994) 4996.
[24] S. Rex, V. Eyert, W. Nolting., J. Magn. Mat. 192 (1999) 529.
[25] B. Sinkovic, E. Shekel, S.L. Hulbert, Phys. Rev. B 52 (1995) R15703.
[26] P.B. Allen, Phys. Rev. B 63 (2001) 214410.
[27] C. Zener, Phys. Rev. 81 (1951) 440;
C. Zener, Phys. Rev. 82 (1951) 403;
C. Zener, Phys. Rev. 83 (1951) 299.
[28] A.V. Fedorov, K. Starke, G. Kaindl, Phys. Rev. B 50 (1994) 2739.
[29] J.R. Schrieffer, Theory of Superconductivity, Bejamin/Cummings Publishing Company, Reading, Massachusetts, 1964.
[30] J.H. Schön, Ch. Kloc, B. Batlogg, Science 293 (2001) 2432.
[31] H.J. Choi, D. Roundy, H. Sun, M.L. Cohen, S.G. Louie, Cond-mat/0111183 (2001).
[32] M. Gurvitch, A.T. Fiory, Phys. Rev. Lett. 59 (1987) 1337.
[33] P.W. Anderson, Proceedings of Fermi International School of Physics, Frontiers and Borderlines in Many-particle Physics, North-Holland, Amsterdam, 1987.
[34] C.M. Varma, P.B. Littlewood, S. Schmitt-Rink, E. Abrahams, A.E. Ruckenstein, Phys. Rev. Lett. 63 (1989) 1936.
[35] V.J. Emery, S.A. Kivelson, J.M. Tranquada, Natl. Acad. Sci. USA 96 (1999) 8814.
[36] C. Kim, J. Elect. Spectros. Relat. Phenom. 117–118 (2001) 503.
[37] (a) P. Bogdanov et al., Phys. Rev. Lett. 85 (2000) 2581;
(b) A. Kaminski et al., Phys. Rev. Lett. 86 (2001) 1070.
[38] A. Lanzara et al., Nature (Lond.) 412 (2001) 510.
[39] M. Hengsberger, D. Purdie, P. Segovia, M. Garnier, Y. Baer, Phys. Rev. Lett. 83 (1999) 592; S. LaShell, E. Jensen, T. Balasubramanian, Phys. Rev. B 61 (2000) 2371.
[40] R.J. Mcqueeney et al., Phys. Rev. Lett. 82 (1999) 628.
[41] J.J. Tu, C.C. Homes, G.D. Gu, D.N. Basov, S.M. Loureiro, R.J. Cava, M. Strongin, cond-mat/0104208 (2001).

[42] P.D. Johnson et al., Phys. Rev. Lett. 87 (2001) 177007.
[43] P. Dai et al., Science 284 (1999) 1344.
[44] H.-Y. Kee, S.A. Kivelson, G. Aeppli, cond-mat/0110478 (2001).
[45] M. Eschrig, M.R. Norman, Phys. Rev. Lett. 85 (2000) 3261.
[46] A. Abanov, A.V. Chubukov, M. Eschrig, M.R. Norman, J. Schmalian, cond-mat/0112126 (2001).
[47] T. Valla, A.V. Fedorov, P.D. Johnson, Q. Li, G.D. Gu, N. Koshizuka, Phys. Rev. Lett. 85 (2000) 828.
[48] A. Kaminski et al., Phys. Rev. Lett. 84 (2000) 1788.